

## Vibrational Band Modes in Germanium: Isotopic Disorder-Induced Raman Scattering

H. D. Fuchs, P. Etchegoin, and M. Cardona

*Max-Planck-Institut für Festkörperforschung, Heisenbergstrasse 1, D-7000 Stuttgart 80, Germany*

K. Itoh and E. E. Haller

*University of California and Lawrence Berkeley Laboratory, Berkeley, California 94720*

(Received 10 November 1992)

We present Raman spectra of natural Ge,  $^{70}\text{Ge}$ , and  $^{70}\text{Ge}_{0.5}^{76}\text{Ge}_{0.5}$  in the TO phonon region. The spectrum of the isotopically pure  $^{70}\text{Ge}$  shows only the Raman-active phonon with  $\vec{k} = 0$  ( $\Gamma$ ), as required by  $\vec{k}$  conservation. The two isotopically disordered crystals, however, show spectra at the low energy side of the  $\Gamma$  phonon which correspond to isotopic disorder-induced scattering by TO phonons with  $\vec{k} \neq 0$  (band modes). The line shape and the strength of the observed spectra agree with calculations based on the coherent potential approximation and an ansatz for the Raman polarizability. The novel  $^{70}\text{Ge}_{0.5}^{76}\text{Ge}_{0.5}$  thus proves to be an ideal crystal to investigate mass disorder effects.

PACS numbers: 78.30.Fs, 63.20.Dj, 63.20.Mt

Effects of isotopic disorder on the vibronic properties (infrared transmission and Raman spectra) of diamond [1, 2] and germanium [3–7] have recently received considerable interest, triggered by the availability of nearly isotopically pure materials [8, 9]. Most of this work has been concerned with the self-energy of the Raman-active phonons at the Brillouin zone center ( $\Gamma$ ). In this Letter we discuss our observation of the isotopic disorder-induced Raman scattering by  $\vec{k} \neq 0$  phonons in natural Ge and the even more isotopically disordered  $^{70}\text{Ge}_{0.5}^{76}\text{Ge}_{0.5}$  alloy. The disorder in these materials involves only fluctuations in the isotopic mass and not in the electronic properties (e.g., the Raman polarizabilities). The isotopic disorder thus represents the simplest kind of disturbance of the translational invariance and is ideally suited for a comparison with theoretical models of the vibrations of alloys. Recent related work for the  $\text{Ge}_x\text{Si}_{1-x}$  alloys [10, 11] postulates strongly simplified models for the Raman polarizabilities, a fact which obscured comparison with theoretical predictions. The effects discussed here should be a paradigm for many crystals grown out of natural (i.e., isotopically mixed) constituents.

The replacement of atoms by impurities can lead to additional vibrational modes in the crystal, to wit:

(i) *Localized modes* (bound states) appear with frequencies above the range of the unperturbed modes if the mass of the impurity is lighter than that of the host. The vibration of heavier impurities cannot be localized at the impurity site because its frequency lies within the continuum of the host material. Such localized modes have been studied in recent years both experimentally and theoretically for a large number of different materials. In Ge, however, the mass difference between the various isotopes (20%  $^{70}\text{Ge}$ , 27.4%  $^{72}\text{Ge}$ , 7.8%  $^{73}\text{Ge}$ , 36.5%  $^{74}\text{Ge}$ , 7.7%  $^{76}\text{Ge}$  in natural Ge) is not large enough to localize the vibrations of the individual isotopes [3–7].

Even in the  $^{70}\text{Ge}_{0.5}^{76}\text{Ge}_{0.5}$  alloy we observed only *one* zone center Raman mode corresponding to the average mass.

(ii) *Band modes* (quasilocalized modes) are perturbed vibrations affected by the presence of the impurity which resonate at frequencies within the continuum in the region of nearly 2-dimensional critical points (sharp edges in the phonon density of states with  $\vec{k} \neq 0$ ) [12, 13]. Such vibrational band modes have been observed in  $\text{Ge}_x\text{Si}_{1-x}$  where the modes become infrared active because of the slightly polar character of the Si-Ge bonds [13]. We will show here that in Ge these resonant band modes appear due to the presence of the various isotopes in the crystal, even though the scattering potential due to the mass defects is not strong enough to localize the  $\Gamma$  phonons.

The Ge sample of natural isotopic composition was cut from a high-purity *n*-type single crystal. The purification and growth of the isotopically enriched *n*-type  $^{70}\text{Ge}$  is described in Ref. [3]. A similar procedure was followed for the  $^{70}\text{Ge}_{0.5}^{76}\text{Ge}_{0.5}$ , starting from the isotopically enriched, purified components. The carrier concentration of the crystals as determined from Hall measurements was insufficient to affect the phonon spectra [4]. The Raman spectra were recorded in a backscattering geometry at liquid nitrogen temperatures using the 568.2 nm line of an  $\text{Ar}^+$  laser. The collected light was dispersed by a DILOR XY triple monochromator and the signal accumulated with a multichannel detection system.

Figure 1 summarizes the experimental results. The Raman spectra of our three Ge crystals are dominated by the zone center Raman peak. Its position is determined mainly by the average isotopic mass, renormalized slightly due to the isotopic disorder in the crystal [3]. Note that we shifted the spectrum of  $^{70}\text{Ge}$  in energy for better comparison. The isotopically pure  $^{70}\text{Ge}$  shows no additional features in the spectral range of the TO

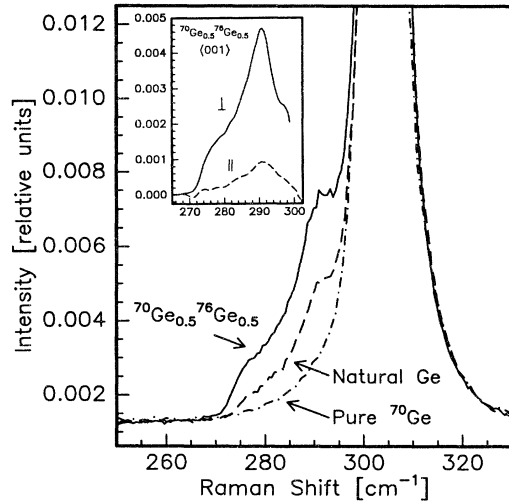


FIG. 1. Raman spectra of isotopically pure  $^{70}\text{Ge}$ , natural Ge, and  $^{70}\text{Ge}_{0.5}^{76}\text{Ge}_{0.5}$  showing the main Raman line at  $304.5\text{ cm}^{-1}$  (off scale) and the isotopic disorder-induced band modes at 80 K. The spectrum of  $^{70}\text{Ge}$  is shifted in energy for comparison. The inset displays the polarization dependence of the band modes in the allowed ( $\perp$ ) and forbidden ( $\parallel$ ) configurations. The data of the inset were obtained by subtracting the main Raman line from the original data. The scattering intensities are normalized so that the peak of the Raman-active mode in the allowed configuration (off scale) is equal to 1.

phonons in Fig. 1. The isotopically disordered Ge crystals, on the other hand, display an additional structure between  $270$  and  $295\text{ cm}^{-1}$  with an integrated intensity of about 2.5% and 0.9% of the  $\Gamma$  peak for  $^{70}\text{Ge}_{0.5}^{76}\text{Ge}_{0.5}$  and natural Ge, respectively. The frequencies of the dominant isotopic disorder-induced features coincide with the sharp edges of the phonon density of states (DOS) in the TO region (Fig. 2) [14]. We thus assign these new features to the band modes of the different isotopes in the crystal, as described above. It is well known that in 2-dimensional systems (steplike DOS at  $\Gamma$ ) mass defects theoretically always lead to bound states (localized modes) even for small mass differences. In the 3-dimensional Ge crystal (parabolic DOS at  $\Gamma$ ) the different isotopes obviously only contribute to an *average*  $\Gamma$ -phonon frequency (main peak in the spectra of Fig. 1). However, the various isotopes manifest themselves as resonant vibrations (band modes) in the continuum near the position of the quasi-2-dimensional critical points in the Brillouin zone near  $X$  and  $L$  (Fig. 2).

In order to compare our experimental results with theory, we calculated the Raman response of mass defects in a crystal with a Green function approach [12, 13]. The intensity of the Raman signal,  $I(\omega)$ , at the frequency  $\omega$  is proportional to the phonon density of states  $\rho(\omega)$  and to the difference between the average of the squared displacements at the impurity site,  $\langle u_{\text{imp}}^2 \rangle$ , and the average

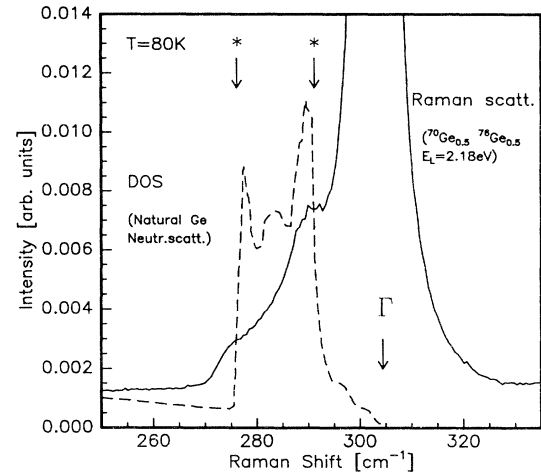


FIG. 2. Raman spectra of  $^{70}\text{Ge}_{0.5}^{76}\text{Ge}_{0.5}$  (solid line) compared to the phonon density of states (DOS, dashed line) at 80 K. The Raman spectra were taken with the 568.2 nm line of an  $\text{Ar}^+$  laser. The dominant band modes (marked with  $*$ ) appear at the edges of the DOS. The scattering intensities are normalized so that the peak of the Raman-active mode at  $\Gamma$  (off scale) is equal to 1.

of the squared displacements of the host,  $\langle u_{\text{host}}^2 \rangle$ :

$$I(\omega) \propto \left| \langle u_{\text{imp}}^2 \rangle - \langle u_{\text{host}}^2 \rangle^{1/2} \right|^2 \frac{\rho(\omega)}{\omega}. \quad (1)$$

The details of the calculations of the phonon amplitudes  $u$  with a Green function method can be found in Ref. [12].

As the simplest case, and to gain some insight in the origin of the band modes in Ge, we calculated the vibrations of one single isotope in an otherwise perfect crystal with average isotopic mass. The Green function in this simple case,

$$G(\omega) \propto \int \frac{\rho(\omega')}{\omega^2 - \omega'^2} d\omega', \quad (2)$$

does not account for any lifetime broadening (anharmonicity, impurity-induced broadening, etc.), and we used the density of states  $\rho(\omega)$  as determined from neutron scattering experiments [14].

In this mean-field approach, the Raman intensity of the Ge crystals can then be expressed as the weighted sum of the contributions from the constituent isotopes. Figure 3(a) shows the respective Raman response of one single  $^{70}\text{Ge}$  and  $^{76}\text{Ge}$  atom within a perfect crystal of average mass  $\bar{m}=73$ . The two spectra were added with equal weight to represent the Raman intensity of  $^{70}\text{Ge}_{0.5}^{76}\text{Ge}_{0.5}$  in Fig. 3(b). The spectrum of natural Ge [Fig. 3(b)] was obtained similarly. It becomes clear from Fig. 3 that the frequency of the impurity modes is mainly determined by the sharp features in the DOS and the principal effect of the isotope mass is only to determine the respective contribution to the lower and higher energy peak. Even in this simple approach, the

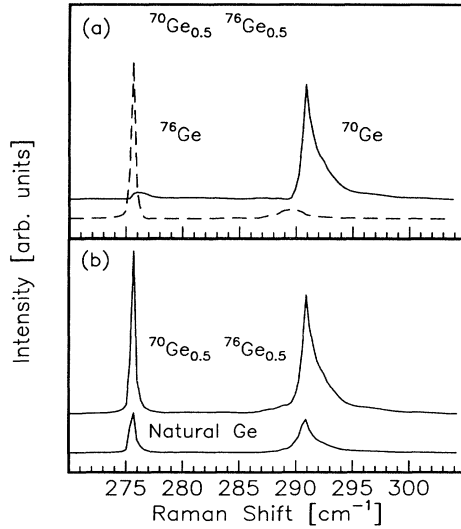


FIG. 3. Calculations of the Raman intensity using an idealized Green function approach. For details see text.

frequencies of the two peaks in Fig. 3 are in rather good agreement with the frequencies of the additional features of the Raman spectra in Figs. 1 and 2.

We obtained a more realistic calculation of the vibrational modes of isotopically disordered Ge using the coherent potential approximation (CPA). We employ the CPA by replacing the idealized Green function of Eq. (2) by the Green function obtained from self-consistent CPA calculations to explicitly take into account the isotopic disorder in the crystals [3]. Also, we used the imaginary part of this self-consistent CPA Green function to describe the DOS in Eq. (1). With the formalism of Dawber and Elliott [12], the phonon amplitudes and the Raman intensities are calculated. Figure 4 compares the so-obtained CPA results with experiment. The calculations represent exclusively the effect of the fluctuations of the isotopes, and not their average, coherent contribution to the  $\Gamma$  Raman mode. For this reason we subtracted a Lorentzian line from the experimental spectra of Fig. 1 in order to compare them with the calculation. The experimental three-peak structure of the Raman intensity in Fig. 4 is well reproduced by the CPA calculations, even though there is some additional scattering in the experiment around  $285 \text{ cm}^{-1}$  which is not taken into account in the calculations.

Not only is the frequency of the observed band modes accurately described by the CPA calculations but also their relative intensity with respect to the main  $\Gamma$  Raman mode. The CPA yields a relative integrated intensity of 2.1% for  $^{70}\text{Ge}_{0.5}^{76}\text{Ge}_{0.5}$  (expt.: 2.5%) and 0.82% for natural Ge (expt.: 0.9%). This means that the band modes in  $^{70}\text{Ge}_{0.5}^{76}\text{Ge}_{0.5}$  are about 2.7 times stronger than in natural Ge and are therefore easier to detect experimentally.

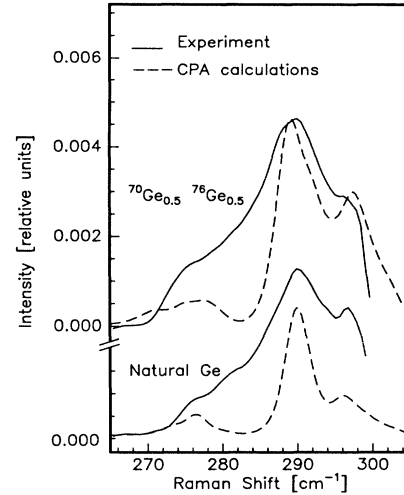


FIG. 4. Raman spectra of the vibrational band modes in  $^{70}\text{Ge}_{0.5}^{76}\text{Ge}_{0.5}$  and natural Ge. The experimental data were obtained by subtracting the main Raman line from the original data of Fig. 1. The calculations are based on the coherent potential approximation (CPA). The spectra of natural Ge are shifted vertically for clarity. The scattering intensities are normalized so that the peak of the Raman-active mode at  $\Gamma$  is equal to 1.

Also of interest is the experimental polarization dependence of the band mode intensity (inset of Fig. 1). In crossed polarizations parallel to the crystal axes ("Raman allowed" for the  $\Gamma$  phonons) the band modes are about four times more intense than in the "Raman-forbidden" configuration (parallel polarizations). The parallel configuration scattering should vanish like the Raman-active  $\Gamma$  phonon within the simple tetrahedral polarizability model used here and in [11]. A description of the weak strength of polarized scattering would require two-site correlations in the isotopic distribution which are beyond the scope of the one-site CPA [11].

In conclusion, we have observed Raman-active *band modes* in natural Ge and in a novel  $^{70}\text{Ge}_{0.5}^{76}\text{Ge}_{0.5}$  crystal. These isotopic disorder-induced TO Raman modes vibrate with frequencies within the continuum and are enhanced close to nearly 2-dimensional critical points, even though the scattering potential of the mass defects in Ge is not strong enough to localize these vibrations. Since the variation in the atomic mass is the only disturbance of the translational invariance in the crystals and no fluctuations in the electronic properties occur, these isotopically mixed materials are ideal systems to study disorder effects. As opposed to cases like  $\text{Ge}_x\text{Si}_{1-x}$ , no strongly simplified models for the Raman polarizability have to be used. For this reason, the CPA as a mean-field approximation accurately describes the vibrational properties of isotopically mixed Ge, with a simple, natural ansatz for the polarizability. The calculated energy positions and intensities of the vibrational band modes

in Ge using CPA are in excellent agreement with experiment.

A detailed analysis of isotopic disorder-induced effects on the phonons and the electronic structure in Ge including photoluminescence, ellipsometry, neutron scattering, infrared transmission, and optical transmission experiments together with extensive calculations will be presented in a future publication.

We acknowledge B. Lederle, M. Siemers, P. Wurster, and H. Hirt for technical support. This work was supported in part by U.S. NSF Grant No. DMR91-15856.

- 
- [1] K.C. Hass, M.A. Tamor, T.R. Anthony, and W.F. Banholzer, *Phys. Rev. B* **44**, 12 046 (1991).
  - [2] K.C. Hass, M.A. Tamor, T.R. Anthony, and W.F. Banholzer, *Phys. Rev. B* **45**, 7171 (1992).
  - [3] H.D. Fuchs, C.H. Grein, C. Thomsen, M. Cardona, W.L. Hansen, E.E. Haller, and K. Itoh, *Phys. Rev. B* **43**, 4835 (1991).
  - [4] H.D. Fuchs, C.H. Grein, R.I. Devlen, J. Kuhl, and M. Cardona, *Phys. Rev. B* **44**, 8633 (1991).
  - [5] H.D. Fuchs, C.H. Grein, M. Bauer, and M. Cardona, *Phys. Rev. B* **45**, 4065 (1992).
  - [6] H.D. Fuchs, C.H. Grein, M. Cardona, W.L. Hansen, E.E. Haller, and K. Itoh, *Solid State Commun.* **82**, 225 (1992).
  - [7] M. Cardona, C.H. Grein, H.D. Fuchs, and S. Zollner, *J. Non-Cryst. Solids* **141**, 257 (1992).
  - [8] V.F. Agekyan, V.M. Asnin, A.M. Kryukov, I.I. Markov, N.A. Rud, V.I. Stepanov, and A.B. Churilov, *Fiz. Tverd. Tela (Leningrad)* **31**, 101 (1989) [*Sov. Phys. Solid State* **31**, 2082 (1989)].
  - [9] W.F. Banholzer, T.R. Anthony, and R. Gilmore, in *Proceedings of the Second International Conference on New Diamond Science and Technology*, edited by R. Messier, J.T. Glass, J.E. Butler, and R. Roy (Materials Research Society, Pittsburgh, 1990), p. 857; W.F. Banholzer and S. Fulghum, in *Proceedings of the International Conference on Optical Science Engineering*, edited by S. Singer (SPIE-International Society for Optical Engineering, Bellingham, WA, 1991), p. 163.
  - [10] C.H. Grein and M. Cardona, *Phys. Rev. B* **45**, 8328 (1992).
  - [11] S. Gironcoli and S. Baroni, *Phys. Rev. Lett.* **69**, 1959 (1992).
  - [12] P.G. Dawber and R.J. Elliott, *Proc. R. Soc. London A* **273**, 222 (1963).
  - [13] S.C. Shen and M. Cardona, *Solid State Commun.* **36**, 327 (1980).
  - [14] G. Nellin and G. Nielsson, *Phys. Rev. B* **5**, 3151 (1972).